# Superconducting properties of a textured NbN film from $^{93}$Nb NMR relaxation and magnetization measurements

A. Lascialfari,[1,2,3] A. Rigamonti,[1] E. Bernardi,[1] M. Corti,[1] A. Gauzzi,[4] and J. C. Villegier[5]
[1]*Dipartimento di Fisica A.Volta, CNR–INFM and Unità CNISM, Università di Pavia, Via Bassi 6, I-27100 Pavia, Italy*
[2]*Dipartimento di Scienze Molecolari Applicate ai Biosistemi, Università di Milano, via Trentacoste 2, I-20134 Milano, Italy*
[3]*S3-CNR–INFM, 41100 Modena, Italy*
[4]*IMPMC, Universitè Pierre et Marie Curie-Paris 6–CNRS, 4, place Jussieu, 75252 Paris, France*
[5]*CEA, INAC, SPSMS, 17 rue des Martyrs, 38054 Grenoble Cedex 9, France*
(Received 30 September 2008; revised manuscript received 27 April 2009; published 9 September 2009)

Primarily motivated by the similarities between the underdoped superconducting cuprates and the granular systems in regards of electric conductivity, phase fluctuations of the order parameter, and nuclear spin-lattice relaxation, a study has been carried out in a NbN(111) textured film at controlled granularity by means of superconducting quantum interference device magnetization and $^{93}$Nb NMR measurements. The Meissner diamagnetism in zero-field-cooling and field-cooling conditions and for different orientation of the magnetic field and the isothermal magnetization curves around the superconducting transition temperature $T_c$, are studied. $^{93}$Nb spectra and relaxation measurements have been performed for two values of the external magnetic field in parallel and perpendicular geometry, in the temperature range 4–300 K. In the superconducting phase the experimental findings for the textured film are similar to the one in bulk NbN. The nuclear spin-lattice relaxation process is the same as in bulk NbN in the temperature range 50–300 K, confirming a dominant contribution to the density of states at the Fermi energy arising from the Nb 4*d* band. At variance, on cooling from about 40 K down to $T_c$ $(H)$, the $^{93}$Nb relaxation rate in the film dramatically departs from the expected behavior for the Fermi gas and mimics the opening of a spin gap. The interpretation of the spin-gap opening in terms of depletion in the density of states at the Fermi energy can justify the anomalous temperature behavior of the $^{93}$Nb relaxation rate on approaching $T_c$ $(H)$ from above. The experimental findings suggest the occurrence of superconducting fluctuations (density-of-states term) in one-dimensional regime, coupled to a reduction in the time of flight of the electrons, both effects being related to the granularity. The data also suggest that the spin-gap phase in underdoped cuprates could be connected more to granularity, rather than to exotic mechanisms of magnetic origin.

DOI: 10.1103/PhysRevB.80.104505 PACS number(s): 74.40.+k, 74.20.De, 74.70.Ad

## I. INTRODUCTION

NbN is one of the most used low-temperature ($T_c \approx 15$ K) superconducting binary compound with high performances in a variety of applications, ranging from high-field magnets to Josephson junctions and microelectronic ultrafast devices based on rapid single-flux quantum elements. The metallic atom Nb and nonmetallic atom N are arranged on NaCl-type lattice, with two interpenetrating fcc lattices, so that each atom of one type is at the center of an octahedron of atoms of the other type. In most samples some percent of vacancies are present, affecting the electric conductivity, among other normal-state and superconducting properties.[1]

Often NbN is created in form of films by reactive sputtering of Nb in a partial pressure of N or by laser ablation of Nb target in $N_2$ environment.[2] Polycrystalline films are usually affected in their transport, superconducting and screening properties by the reduction in the coherence length, besides by the structural imperfections and granularity, as expected.

In NbN cermets the effects of granularity on the superconducting properties can be studied with a fine control over the structure of the films. Cermets are microgranular mixtures of metallic and insulating particles prepared by reacting radio frequency (rf) sputtering and NbN cermets with regular grains in a matrix of Nb oxide or of Boron nitride have been studied since a long ago.[3,4] Superconducting (SC) samples of that type in general have resistivity increasing with decreasing temperature according to a logarithmic relation of the form $\rho(T)=\rho_0 \ln(T_0/T)$. In the vicinity to the transition to the SC state occurrence of fluctuations of Aslamazov-Larkin character has been evidenced.[4] Thus, wide-ranging logarithmic temperature dependence of $\rho(T)$ and Kosterlitz-Thouless phase transition could be considered the characteristic feature of SC films with well-controlled granularity. Resistivity around 200 $\mu\Omega$ cm, with tendency to increase on cooling toward $T_c \approx 15$ °K and displaying fluctuation conductivity according to Aslamazov-Larkin model was recently pointed out from microwave measurements in NbN films deposited on $LaSrAlO_4$ (001) substrate by reactive sputtering technique.[5]

It can be emphasized that granularity with tunable parameters is believed the crucial property in order to understand the interplay between electron correlation and disorder and the related metal-insulator and SC-insulator transitions. The theory of SC transition in granular systems, based on the Ginzburg-Landau scenario for the grains and Josephson coupling among the grains, was initiated by Deutscher *et al.*,[6] pointing out a variety of crossover effects depending on the granular "structure." The most recent theoretical work attacking the role of granularity and disorder in SC compounds

 

from the point of view of the fluctuations is the one from Lerner, Varlamov, and Vinokur.[7]

The temperature dependence of the resistivity and the SC fluctuations in granular NbN films with crossover between different dimensional regimes, has suggested to study these systems also in the attempt to get insights on the underdoped phase of high-temperature SC cuprates. As it is known, remarkable deviations from Fermi-liquid behavior occur in that phase, often interpreted in terms of a pseudogap (PG) phase opening up well above $T_c$. Although in general terms the PG opening is essentially a transfer of spectral weight from the low energy to the high energy range, the real nature of the underdoped phase in cuprates and the under-lying physical mechanism are still elusive, in spite of the large number of experimental and theoretical efforts.[8,9] It is even possible that PG and the SC gap arise from different mechanisms,[10] even though an opposite interpretation has been claimed.[11] We will simply recall here, for the use in the forthcoming discussion, that from a phenomenological point of view the PG phase, in the terms revealed from the temperature dependence of the nuclear spin-lattice relaxation rate,[12] appears to be concomitant with "anomalous" resistivity resembling the logarithmic temperature dependence in granular films.[13]

Remarkably, another similarity suggesting a connection of the PG phase in underdoped cuprates with granular systems, involves the mechanism of phase fluctuations of the order parameter above $T_c$. As pointed out on the basis of isothermal diamagnetic magnetization measurements[14] and by vortexlike Nernst signal,[15] in underdoped cuprates one finds regions above the bulk $T_c$ where the order parameter is different from zero while phase fluctuations prevent the coherence granting long-range order and existence of a stable SC state.

In this respect a stimulating experimental observation in NbN films was provided by Lamura *et al.*[16] From the low-temperature dependence of the magnetic penetration depth $\lambda$, evidence of granularity-induced gapless *s*-wave superconductivity was provided in thick (111) textured NbN films having $T_c$ close to the bulk compound and with almost flat temperature dependence of resistivity. Ruling out the role of magnetic impurities and proximity effects, from the linear increase in $\lambda(T)$ phase fluctuations of the order parameter were inferred.[16–18] It is worthy to note that the interpretation of the experimental data was given by Lamura *et al.*[16] by assuming an array of SC grains with intergranular Josephson coupling. This implies in the Ginzburg-Landau functional a term of the form $J\Sigma_{i\neq j}[1-\cos(\theta_i-\theta_j)]$ (where $\theta_i$ is the phase in the $i$th grain), strictly similar to the one assumed[14,19] in order to explain the fluctuating diamagnetism in underdoped SC cuprates (here the summation is over the $CuO_2$ planes, with $j=i+1$). The granularity-related SC fluctuations similar to the ones in cuprates could be present also above $T_c$ in thick (111) textured NbN films.

Motivated by the afore mentioned scenario we have carried out a study of the NMR spin-lattice relaxation and the diamagnetic properties in one *ad hoc* NbN film prepared in order to exhibit resistivity close to a logarithmic temperature dependence and phase fluctuation of the order parameter in the low-temperature range. In this report the results of high-resolution superconducting quantum interference device (SQUID) magnetization measurements and of $^{93}$Nb NMR relaxation are presented.

The paper is organized as follows. After some experimental aspects and characterization data of the sample (§2), the experimental results of the diamagnetic magnetization and of $^{93}$Nb NMR line and spin-lattice relaxation rate, are presented at §3. After recalling the nuclear-relaxation mechanism and the fluctuating diamagnetism expected for ideal Fermi gas of carriers, a thorough discussion of the results along the afore mentioned lines is given at §4. It is pointed out, in particular, how in the (111) textured film in a wide temperature range above $T_c$ $(H)$, the $^{93}$Nb relaxation rate $2W$ exhibits a dramatic departure from the behavior expected for ordinary metal and already observed in bulk NbN. The temperature dependence of $2W$ can be read as PG opening for $T\leq 3$ $T_c$ (0) and the possible sources of such unexpected result are discussed in terms of some mechanisms leading to it. It turns out that the term of SC fluctuations implying a decrease in the density of states due to metastable pairing (DOS term, see Ref. 20) can account for the experimental observation of $2W$. The implications in regards of the underdoped phase of cuprates SC are addressed. Summarizing remarks and conclusions are collected at §5.

## II. EXPERIMENTAL ASPECTS

The NbN film used in the present study is a (111) textured layer grown onto $Al_2O_3$ substrate by dc magnetic sputtering at room temperature, of properties strictly similar to the one described in Ref. 16. The NbN films are dc-magnetron sputtered from a high purity, 6 inch diameter Nb target in a reactive mixture of argon and nitrogen gas, leading to good thickness uniformity on 3 inch diameter substrates. Argon gas flow is kept constant during the presputtering and sputtering while the flow of nitrogen is self-adjusted in order to maintain the total gas pressure constant. The NbN base electrodes are about 300-nm thick and are deposited at 300 °C while the counterelectrodes are 450-nm thick, the substrate being at room temperature. Background pressure is $2.6\times10^{-5}$ Pa before deposition. Deposition rates of about 3 $nms^{-1}$ are obtained for a gas pressure of 1.97 Pa with a constant flow ratio. The critical temperatures are $T_c\sim 15$ K for both electrodes while film resistivities are in the range 180–450 $\mu\Omega$ cm, measured at 20 K.

On the average the grain size is $d\approx 100$ Å while the intergranular space, composed primarily by Nb oxides is around 10–20 Å. The dc resistivity at $T=300$ K is around $\rho=100$ $\mu\Omega$ cm and on cooling it displays a slight increase on approaching the transition temperature.

From magnetic-susceptibility measurements (see subsequent data) in small field the superconducting transition temperature turns out $T_c(0)\approx 15\pm 0.1$ K, close to the one in well-prepared bulk NbN ($T_c\approx 15.2$ K) and indicating the absence of sizeable amount of impurities and/or defects. Since the superconducting transition temperature and the Meissner fraction were found to be slightly different for samples cut in different region of the original disk of the substrate, for precise measurements we had to reduce the sample size to about 5 mm$\times$5 mm. The magnetization

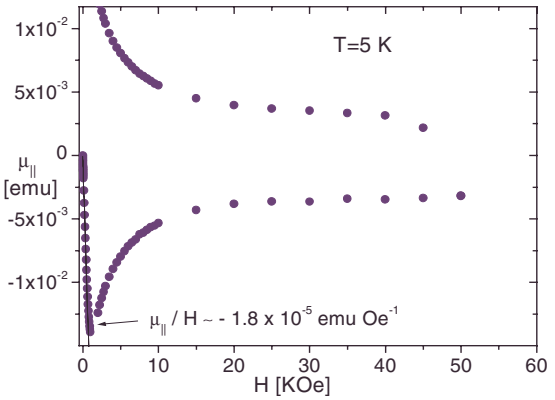


FIG. 1. (Color online) Magnetization of NbN film as a function of the external field applied along the plane, at $T=5$ K.

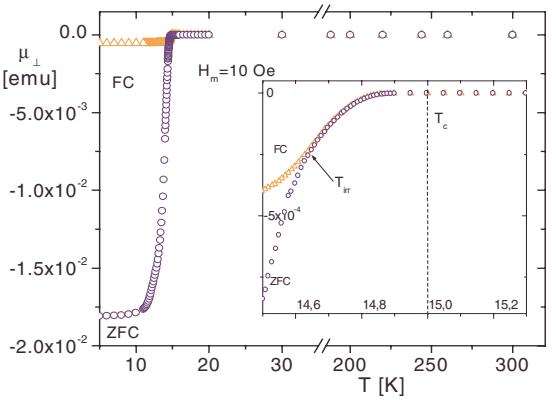


FIG. 2. (Color online) Temperature dependence of the magnetic moment of the NbN film, for measuring field perpendicular to the layer. In the inset the blow up of the data around $T_c \approx 15$ K and the indication of the irreversibility temperature are shown.

curve at $T=5$ K (see Sec. III A) indicates an effective SC volume of the film around $1.9\times10^{-4}$ cm$^3$, corresponding to a thickness of about $7\times10^{-4}$ cm. Susceptibility data indicate a decrease in $T_c$ with increasing magnetic field similar to the one measured for bulk NbN (see subsequent data).

The magnetic susceptibility as a function of temperature and the isothermal magnetization curves have been measured by means of Quantum Design SQUID magnetometer, with high-temperature resolution, by applying the external magnetic field along the plane of the film and perpendicular to it. The diamagnetic magnetization around the superconducting transition was obtained by a subtraction procedure, by eliminating from the raw data the Pauli paramagnetic contribution measured as a function of the field a few degrees above $T_c$.

Standard NMR pulse techniques with Fourier transform (FT) have been used to derive the line width, the resonance shift, and the spin-lattice relaxation rate in the temperature range 4–300 K, for two values of the external magnetic field $H_0$, namely, $H_0=7.5$ T and $H_0=3.8$ T, applied parallel and perpendicular to the film. A few data collected in samples having $T_c(0)$ slightly different (see above) did not show any difference in the NMR aspects.

In the high-temperature range the NMR signal was very weak and sometimes up to $10^4$ acquisitions were required in order to achieve workable signal to noise ratios in the relaxation measurements. Below about 50 K the number of acquisitions for reliable relaxation measurements could be reduced to 400, for each echo signal following a given delay from the saturating comb.

## III. RESULTS

### A. Susceptibility and isothermal magnetization curves

In Fig. 1 the magnetization curve of the sample at $T=5$ K and for magnetic field applied along the plane of the film, is reported. Two significant deductions can be drawn. Since the Meissner fraction in bulk NbN is close to 100%, from the diamagnetic susceptibility of the film $(\mu_\parallel/H)\approx -1.8\times10^{-5}$ emu Oe$^{-1}$ (for $H<1000$ Oe) the effective SC volume is found $V=1.9\times10^{-4}$ cm$^3$, as already reported. Furthermore, from the results in Fig. 1 the lower critical field $H_{c1}$ appears around 1000 Oe and again in comparison to the data in bulk NbN (in the assumption of demagnetization factor for spherical particles, data not reported) the demagnetization factor for our sample is confirmed very close to zero for parallel orientation, as expected.

In Fig. 2 the temperature dependence of the magnetic moment of the film $\mu_\perp$, for measuring external field $H_m=10$ Oe perpendicular to the plane, is reported for zero-field cooling (ZFC) and field-cooling (FC) conditions. In the perpendicular geometry the SQUID signal at low temperature is increased by a factor more than 100, consistent with the demagnetization factor strongly increasing the effective field. This can be considered an indication of the good film quality in regards of the superconducting properties. The blow up of the data for the magnetic moment $\mu_\perp$ in weak field around the SC transition, is reported in the inset of Fig. 2. The comparison of the FC and ZFC data indicate an irreversibility temperature $T_{irr}=14.65$ K.

The magnetic moment $\mu_\parallel$ for magnetic field along the plane (so that the effective field practically coincide with $H_m$), is reported around the transition, for different strength of the field, in Fig. 3. In Fig. 4 the isothermal diamagnetization curves for temperature around $T_c(0)$ are shown. As reported in the inset the upturn field $H_{up}$, defined as the field at

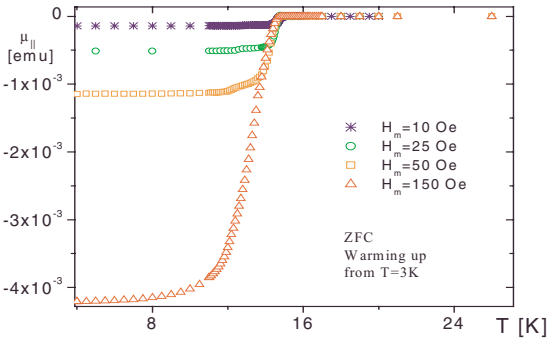


FIG. 3. (Color online) Temperature dependence, around the transition temperature, of the magnetic moment measured for different field $H_m$ aligned along the plane of the film.

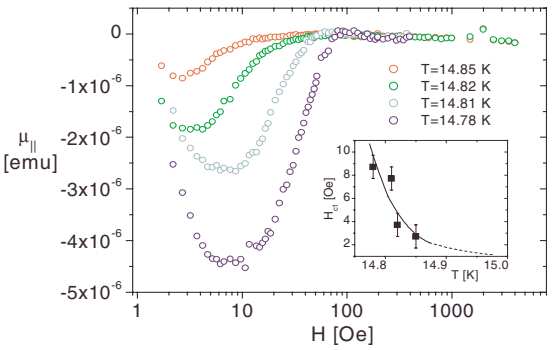


FIG. 4. (Color online) Magnetization curves around the transition temperature. In the inset the temperature dependence of the upturn field (practically coinciding with the critical field $H_{c1}$, see text), is reported (the line is a guide for the eye).

which the diamagnetic magnetization initiates to decrease on increasing field, increases on decreasing $T$. Therefore, according to the observations in other SC systems,[21] $H_{up}$ in the NbN film studied here is not the field related to the quenching of the fluctuating Cooper pairs[20] but rather tracks the temperature dependence of the critical field $H_{c1}$. This attribution is supported by the observations in Nb metal as well as from our measurements in bulk NbN. The magnetization curve around $T_c+0.1$ K in a large sample of bulk NbN (data not reported) indicate $H_{up}$ around 300 Oe, increasing on increasing temperature. From the magnetization curves evidence of sizeable enhancement in the fluctuating diamagnetism (FD) above $T_c$ is lacking. One has to remark that in the absence of enhancement of the type detected in underdoped cuprates and attributed to phase fluctuations,[14] the expected conventional FD should give a SQUID signal hard to detect, due to the smallness of the effective sample (see discussion in Sec. V).

### B. $^{93}$Nb spectra

The envelope of the amplitude of the echo following a pair of pulses as a function of the rf, in a field $H_0 \approx 7.5$ T and for pulse length of about 5 $\mu$s, is reported in Fig. 5(a). This broad spectrum, as well as the length of the pulses maximizing the echo signal (about 2 $\mu$s) indicate that the local symmetry at the Nb site is not cubic for a large part of the nuclei. The electric field gradient (EFG) causing the first-order perturbation to the pure Zeeman states is likely to be most due to the grain boundaries. It is conceivable that the two shoulders in the spectrum, separated by $\Delta\nu \approx 1.6$ MHz, approximately correspond to the first satellite components. By assuming for simplicity that the local symmetry of the EFG does not differ much from the cylindrical symmetry and that the lines are predominantly due to nuclei where the $V_{zz}$ component of the EFG tensor is perpendicular to the applied magnetic field, then the shift of the first satellite line is given by

$$\nu_m^{(1)} \approx -(m-1/2)\nu_Q \quad \text{with} \quad \nu_Q = 3e^2qQ/2I(2I-1)h = \\ = e^2qQ/24\ h.$$

Thus, from $\Delta\nu \approx \nu_Q$, the order of magnitude of the quadrupole coupling constant ($e^2\ qQ/h$) can be estimated around 38 MHz. For the quadrupole moment $eQ$ of the Nb nuclei this value is the one expected in moderate strength of the EFG.

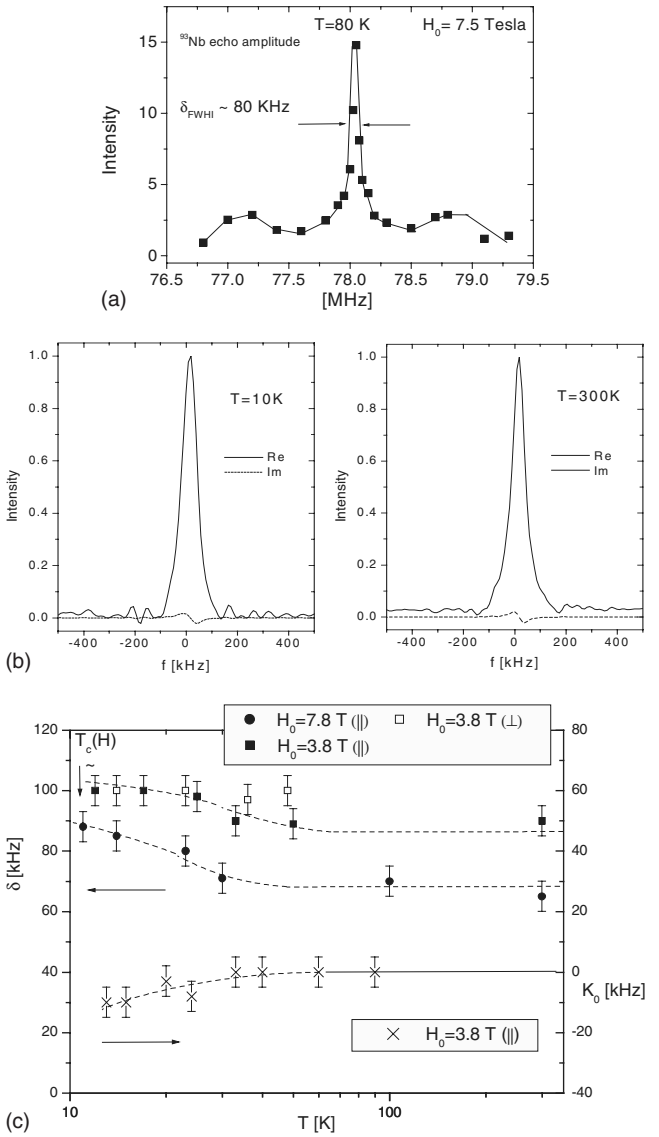


FIG. 5. (a) $^{93}$Nb NMR spectrum at room temperature obtained from the envelope of the echo amplitude as a function of the rf frequency, in a field of 7.5 T. (b) direct FT of half of the echo signal of the central line, at two representative temperatures, where the (sampled) experimental points are connected by a line. (c) line width $\delta$ (at the two values of the magnetic field) and resonance shift $K_0$ as a function of temperature. The wings are simply the FT of the baseline noise and/or of small "ringing" that follows the pulses and they have no effect on the relaxation measurements at high temperature. For $K_0$ the shift in the low-temperature range is reported with respect to the one ($\approx -2\times10^{-2}$% with respect to the theoretical value for bare nucleus) measured in the high-temperature range (see text). The dashed lines are guide for the eye.

From the wide-line spectrum in Fig. 5(a) the full width at half intensity (FWHI) $\delta$ of the central line appears around 80 kHz. A more precise estimate of $\delta$ is obtained from half of the echo signal, by taking into account the second-order

broadening by the quadrupole interaction of the NMR central line, as it will be shown in the following.

For cylindrical symmetry of the EFG and a given angle $\theta$ between $V_{zz}$ and $H_0$ the second-order shift of the central line is

$$\nu_{1/2}^{(2)} \approx -(\nu_Q^2/16\ \ \nu_L)[I(I+1)-3/4](1-\cos^2\theta)(9\cos^2\theta-1). \tag{1}$$

For $\theta=\pi/2$ and $\nu_Q \approx 1.5$ MHz this equation would imply a shift around 50 kHz. In the assumption of a Gaussian-type spectral distribution this corresponds to $T_2^* \approx 2(\ln 2)^{1/2}/\pi\delta \approx 10\ \mu$ sec. Further mechanism of broadening make hard to evidence the free induction decay (FID) signal.

The echo signal of the central line was maximized by two rf pulses of the same length (4 $\mu$s), thus confirming that the main source of the spread of the resonance frequency is of electric-quadrupole character. Other mechanism of broadening can be due to anisotropic Knight shift or to a certain distribution of the demagnetization factors. In bulk NbN, according to the data from Nishihara *et al.*,[22] the shift of the resonance frequency is around $3\times10^{-2}$ percent. In our NbN film the expected distribution of Knight shifts and of demagnetization factor should be smaller than in a distribution of macrograins as in bulk samples. The nuclear dipolar broadening of the line, according to the Van Vleck second moment, is expected on the order of a few kHz.

In Fig. 5(b) the FT of half of the echo signal are reported at two representative temperatures. The FID decay of the central component and therefore the decay of half of the echo signal (detected in quadrature with the rf field) is given by

$$S(t) = \int \cos 2\pi\nu_{1/2}^{(2)} t \sin\theta d\theta d\phi, \tag{2}$$

where $\nu_{1/2}^{(2)}(\theta,\phi,\eta)$ is the second-order quadrupole correction to the Zeeman levels.

The actual shape of the signal depends on the anisotropy parameter $\eta$ of the EFG tensor. However for $\eta \approx 0$ (cylindrical symmetry) the decay $S(t)$ is rather well described by a Gaussian function.[23] The fact that the FT spectra of half of the echoes in Fig. 5(b) are rather well fitted by Gaussian shape can be considered a support to the assumption of EFG's only slightly departing from the cylindrical symmetry. Thus from Eq. (2) one can write for the FID or half of the echo signal

$$S(t) = S(0)\exp[-\alpha^2 t^2/2], \tag{3}$$

where $\alpha^2$ is the second moment in the distribution of the resonance frequencies

$$f(u) = (1/\alpha\sqrt{2\pi})\exp[-u^2/2\alpha^2] \quad (u \text{ and } \alpha \text{ are in rad s}^{-1}).$$

From the second-order quadrupole distribution of the central line $\nu_{1/2}^{(2)}(\theta,\phi,\eta)$, the dephasing time of the echo signal in Eq. (3) is given by[23]

$$\tau_Q \approx 3\ \ R_\eta \nu_L/\pi[I(I+1)-3/4]\nu_Q^2 \tag{4}$$

with $R_\eta \approx 3$.

From the analysis of the echo signal (or equivalently from their FT's) on the basis of Eq. (4), the value of the quadrupole frequency is obtained. One has $\nu_Q=1.1$ MHz, an estimate more precise than the one indicated by the envelope of the echo amplitudes, still confirming the attribution of the two shoulders in Fig. 5(a) as due most to the first satellite lines.

The temperature dependence of the central line width (obtained from FT of half of the echoes) is reported in Fig. 5(c). It is noted that the line width is increased in the lower magnetic field, in agreement with Eqs. (1) and (4) for the contribution related to the distribution of second order quadrupole effects. In the same figure the data for the Knight shift $K_0$ are reported. Due to the small value of $K_0$ (around −8 kHz, at room temperature, with respect to the theoretical value for bare nucleus) compared to the line width, absolute estimates with good accuracy were difficult. Thus we decided to derive the shift in the low-temperature range just from comparison of the spectra with the ones in the high-temperature range.

As it appears from the data in Fig. 5(c), small temperature dependence of the line width and of $K_0$ are possibly present only in the temperature range $T_c(H) < T \leq 35$ K, where a departure from the linear temperature dependence of the relaxation rate occurs [see Subsection (*c*)]. Above about 40 K the line widths and the shift in our NbN film are similar to the one in bulk NbN (see Ref. 22), both being practically temperature independent.

### C. Spin-lattice relaxation rate

In the presence of static quadrupole effects on the Zeeman level implying distribution of resonance lines over several MHz, accurate spin-lattice relaxation measurements are usually difficult. The recovery law, derived from the master equations for the statistical populations over the ten Zeeman levels for $I=9/2$, predicts that the recovery plot $y(t)=[s(\infty)-s(t)]/s(\infty)$, where $s(t)$ is the amplitude of the echo signal after a given sequence of rf pulses modifying the equilibrium distribution, is given by

$$y(t) = \sum_i c_i \exp[-a_i 2\ \ W\ t] \tag{5}$$

a combination of five exponentials involving the fundamental relaxation rate $T_1^{-1}=2$ W and coefficients $c_i$ depending from the initial conditions at $t=0$ and from the relaxation mechanism. For magnetic relaxation mechanism and initial condition corresponding to the complete saturation of all the lines, in principle the recovery plot is characterized by a single exponential, with time constant $2W$. Unfortunately, as it is common for a broad distribution of resonance lines, this convenient situation is usually hard to achieve, even with a very long comb of rf pulses.[24]

For saturation of the central line ($+1/2 \Leftrightarrow -1/2$ transition) only by means of a few rf pulses separated by a time interval larger than the spin-spin relaxation time $T_2$, the recovery plot is characterized by the following coefficients and time constants:

$$c_1 = 7\times10^{-3} \quad \text{for} \quad a_1=1;\ c_2 = 33.5\times10^{-3} \quad \text{for} \quad a_2=6;$$
$$c_3 = 91.8\times10^{-3} \quad \text{for} \quad a_3=15;\ c_4 = 0.192 \quad \text{for} \quad a_4=28;$$
$$c_5 = 0.652 \quad \text{for} \quad a_5=45.$$

Since $c_4$ and $c_5$ dominate, one has a fast initial recovery and the absolute value of $T_1$ is not very reliable, as already ob-

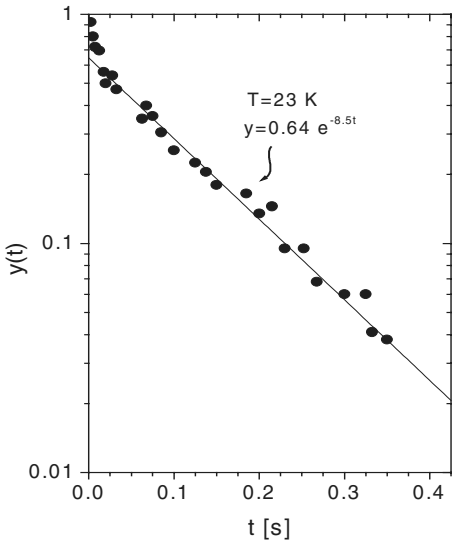


FIG. 6. Typical recovery plot after an almost saturating comb of 100 rf pulses, for $H_0=3.8$ T.

served in bulk NbN.[22] Thus we carried out the relaxation measurements for two initial conditions: (i) one following a few rf pulses saturating the central transition only and (ii) the second after 100 rf pulses separated by 450 $\mu$s, that was found to approach the condition of full saturation. From the comparison of the two plots and most relying on the long times component described by the exponential with time constant $2W$, reliable estimate of the relaxation rate could be obtained, particularly below about 50 K where the Nb NMR signal has a significant increase (see the illustrative recovery plot in Fig. 6). The difference between our data and the ones by Nishihara *et al.*[22] for $T \geq 50$ K is small and systematic and likely to be related to the different method to analyze the recovery plot. If our method is applied to the recovery shown in Fig. 6a of Ref. 22, a total coincidence of the our data with the one from Ref. 22 would be found, for $T \geq 40$ K. It should be noticed also that Eq. (5) has general validity. The changes in the irradiation sequence and/or in the detection, correspond to modify the $c_i$ values while the eigenvalues $a_i$ remain the same. Playing with the two sequences of irradiation described above we could extract the reliable value of $2W$ (the basic relaxation rate, as it is illustrated in Fig. 6). We point out that in any case no difference was noticed in the estimate of $2W$ for bulk or film, unless in the temperature range $T < 40$ K.

The data for $2W$ as a function of temperature are shown in Fig. 7, for the two values of the magnetic field and for parallel and perpendicular geometries. It is noted that in the high-temperature region $2W$ increases linearly on increasing temperature, as expected for the Fermi gas and experimentally found over the whole ordinary state in bulk NbN. On the contrary, on cooling toward $T_c$ ($H_0=7.5$ T) $\approx 11$ K down from about 40 K, a significant departure with respect to the Korringa law and at variance with bulk NbN, is observed in our NbN(111) textured film.

## IV. ANALYSIS OF THE DATA AND DISCUSSION

First one can remark the high quality of the NbN film used in the experiment. The superconducting transition temperature is close to the best NbN bulk samples, the Meissner fraction appears near the ideal one, the irreversibility temperature is just below $T_c$ and finally the transition is sharp. Only small differences in $T_c$ (within about 0.4 degree) have been found in samples cut from different parts of the original disk of the $Al_2O_3$ substrate with the film grown onto it. No evidence of paramagnetic impurities is noticeable from the magnetization data in the ordinary state. No structural phase transitions are detected from the static quadrupole effects and the $^{93}$Nb NMR line width on varying the temperature down to 4 K. The indirect estimates of the demagnetization factors from the magnetic moment measured with field parallel and perpendicular to the slab are consistent with a well-shaped layer of SC NbN.

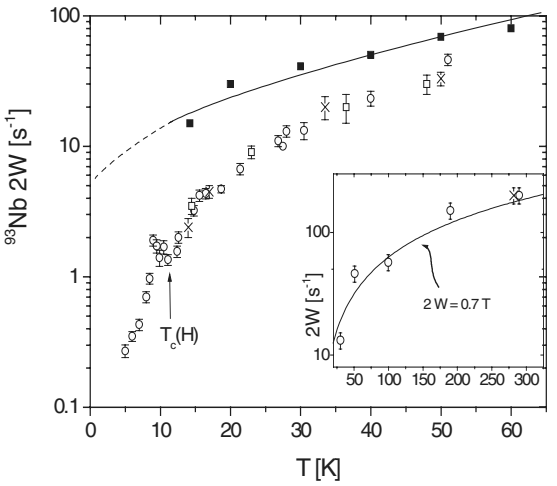


FIG. 7. $^{93}$Nb spin-lattice relaxation rate as a function of temperature in NbN film for $H_0=7.5$ T and perpendicular geometry (○) and $H_0=3.8$ T, perpendicular (x) and parallel geometry (□). For comparison representative experimental data obtained by Nishihara *et al.* (Ref. 22) in bulk NbN of quality similar to our film are reported (■). The difference by a factor 2 of the data in film with respect to the ones in bulk NbN for $T \geq 40$ K is only due to the difference method of derivation of 2 W from the recovery. In the inset it is shown how for $T \geq 40$ K the temperature behavior of 2 W is the one expected for the Fermi gas (Korringa law).

The isothermal magnetization curves measured on approaching $T_c$ from above seem to reveal conventional FD, as the one described by the standard Ginzburg-Landau theory. Looking for a possible evidence of enhancement in the FD similar to the one occurring in the underdoped phase of SC cuprates and attributed to phase fluctuations[14] one has to pay attention to the sensitivity of the SQUID apparatus, in view of the volume of the SC NbN in the film. In fact, the universal value of the fluctuation-induced reduced magnetization

$$m(T=T_c) = -M_{dia}/H^{1/2}T_c$$

is expected $-4.7\times10^{-7}$.[25] For a field $H=100$ Oe, scaling $M_{dia}$ per unit volume to the one for the volume of our sample, the ordinary fluctuation-related diamagnetic moment close to $T_c$ should be around $10^{-8}$ emu. Only in the presence of an enhancement factor as observed in underdoped $YBa_2Cu_2O_{7-x}$ (YBCO) and $La_{2-x}Sr_xCuO_4$ (Ref. 14) (where

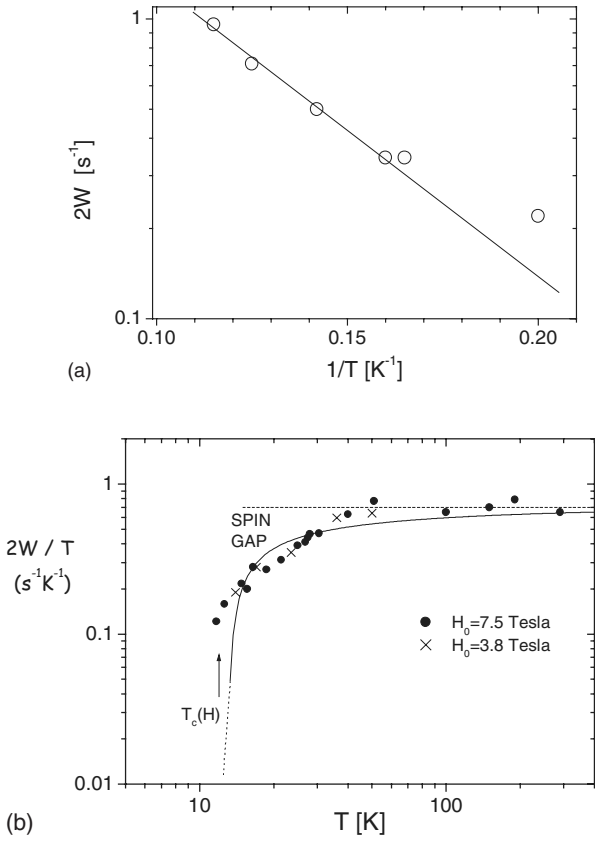


FIG. 8. (a) Relaxation rate below $T_c$ as a function of the inverse temperature, showing the validity of the BCS behavior with a gap around 20 K, namely about 3.5 $T_c(H)/2$; (b) the opening of a pseudospin gap evidenced from $2W/T$ vs $T$; the solid line tracks the theoretical behavior according to Eq. (14), practically with no adjustable parameter. One should remark that for $T \gg T_c$ (H) the 1D condition is only approximate while close to the transition one enters in the critical region and the divergence of the term in $\varepsilon^{-1/2}$ in Eq. (14) is cut off. The dotted line is the behavior expected in accordance to the Korringa law and with no occurrence of spin gap.

also the anisotropy contributes to the enhancement of reduced magnetization) we would be over the limit of our SQUID sensitivity. On the other hand, to increase the measuring field would not help since above about 100 Oe quenching of the fluctuating Cooper pairs is expected, as indicated from the measurements in bulk NbN. In conclusion, enhancement of FD due to phase fluctuation on the order of magnitude of the one occurring in underdoped cuprates is not evidenced in the isothermal magnetization curves above $T_c$ in our NbN film.

Some NMR quantities, such as spectra and resonant shifts, do not appear much different with respect to bulk NbN, with the possible exclusion of a temperature range of about 20 K above $T_c(H) \approx 11$ K [see Fig. 5(c)]. The relaxation data in the SC state [Fig. 8(a)] and just below $T_c$ are consistent with the behavior expected for $s$-wave BCS superconductors. The departure from the conventional scenario of typical ordinary metals appears only in the spin-lattice relaxation data in the temperature range $T_c(H) < T \leq 40$ K, where a spin gap arises [see Fig. 8(b)].

Let us briefly recall, in a form appropriate to the subsequent discussion, the relaxation mechanism from electron scattering by the nuclei[26] as pertinent to the Fermi gas in metals and BCS superconductors, which rather well applies to bulk NbN. The relaxation rate is conveniently expressed in terms of the generalized dynamical susceptibility

$$2W = (\gamma_n^2/2N)k_B T \sum_{\mathbf{k}} [A_{\mathbf{k}}^2 \chi''_{+,-}(\mathbf{k}, \omega_L)/\omega_L]_\perp \quad (6)$$

($\perp$ meaning perpendicular to the quantization axis of $H_0$).

The FT of the hyperfine interaction is little $\mathbf{k}$ dependent for delocalized electrons and then $A_{\mathbf{k}} \approx A$ in Eq. (6) is the scalar contact term. By integrating the generalized susceptibility over the Brillouin zone one has

$$\sum_{\mathbf{k}} [\chi''_{\pm}(\mathbf{k}, \omega_L)/\omega_L]_\perp = (h/2\pi)\rho^2(E_F) \quad (7)$$

[with $\rho(E_F)$ density of states at the Fermi energy]. Thus

$$2W = (64/9)\pi^3 (h/2\pi)^3 \gamma_e^2 \gamma_n^2 \langle |\phi_{\mathbf{k}}(0)|^2 \rangle_F^2 \rho^2(E_F) k_B T \quad (8)$$

namely the Korringa law, often written

$$2W = (8\pi^2 k_B T/h)(\gamma_n/\gamma_e)^2 K_0^2 \quad (9)$$

in terms of the Knight shift $K_0 = (8\pi\chi_P/3)\langle |\phi_{\mathbf{k}}(0)|^2 \rangle_F \Omega$, where $\langle |\phi_{\mathbf{k}}(0)|^2 \rangle_F$ is the average value of the probability density at the nucleus for the electrons near the Fermi level, $\Omega$ is the volume of the unit cell, and $\chi_P$ is the Pauli susceptibility.

Below $T_c$, according to BCS theory and consistently with the decrease in $K_0$ according to the Yoshida function $Y(T) = (\chi_{SC}/\chi_P)$, the relaxation rate goes as $2W \propto \exp[-\Delta(T)/T]$, with the so-called Hebel-Slichter peak just below $T_c$. All the above recalled aspects and the related relaxation mechanisms are well obeyed in bulk NbN as well as in the NbN film for $T > 40$ K. In the ordinary state, as already noticed by Nishihara *et al.*[22] and a long ago by Ehrenfreund and Geballe,[27] the conventional relaxation mechanism for metals is operating. It can be remarked that in this last paper the value $2W = 0.2$ T is probably related to a sample with poor stoichiometry. In our NbN film, as well in bulk NbN,[22] in the high-temperature range one has $2W \approx 0.7$ T [see Fig. 8(b)]. According to this value for the Korringa constant, by using for the hyperfine field due to $s$ electron $h_{5s} = 2.5 \times 10^6$ Oe,[28] the density of $5s$ niobium states per atom at the Fermi energy is around 20% of the total density of states, still leaving a major contribution from the $4d$ Nb band, as deduced from Ehrenfreund and Geballe.[27]

In the SC state, the BCS behavior of $2W$ is found also in the NbN film, with $2\Delta/T_c(H) \approx 3.5$ [see Fig. 8(a)]. Thus we are left to discussing the anomalous behavior of $2W$ observed in the NbN film below 40 K, on approaching the transition to the SC state. At this aim we factorize $[\chi''(\mathbf{k}, \omega)/\omega]$, in the limit $\omega \to 0$ in Eq. (6), in the form $[\chi(\mathbf{k}, 0)/\Gamma_{\mathbf{k}}]$, with $\Gamma_{\mathbf{k}}$ decay rate and $\chi(\mathbf{k}, 0) \approx \chi(0, 0) = \mu_B^2 \rho(E_F)$ according to mean-field arguments. Then

$$2W = BT\chi(0,0) \sum_{\mathbf{k}} \tau_{\mathbf{k}} \quad (10)$$

with $B$ constant. Here $\Sigma_{\mathbf{k}} \tau_{\mathbf{k}}$ is an average correlation time, on the order of the time the electron spends in the vicinity of an atom, namely, on the order of $\tau \approx (h/2\pi)/E_F$. The modifica-

tion in $2W$ vs $T$ below 40 K can be attributed to the quantity $\chi(0,0)\Sigma_{\mathbf{k}}\tau_{\mathbf{k}}$. In the following we discuss some mechanisms that in principle could be responsible for anomalous behavior of the effective correlation time or of the static susceptibility.

### A. quantum size of the grain

The separation between electronic levels in a grain of volume $V$ is on the order of

$$\Psi = 2h^2\pi^2/(6m)Vn^{1/3}$$

and for electrons per unit volume $n \approx 10^{23}$ cm$^{-3}$ and $V = 1.9 \times 10^{-4}$ cm$^3$, and $\Psi$ is negligible compared to $k_B T_c$.

### B. weak localization

In principle one could expect the granularity-induced weak localization, with the decrease in the conductivity below the classical one and thus corresponding to a decrease in the effective correlation time in Eq. (10). Usually, the weak localization correction to Drude conductivity is very small, even in thin films, on the order of $10^{-4}$ and should not be considered as a possible source of the spin-gap opening. However, an intriguing observation involves the role of the external magnetic field. In NbN films of properties similar to our sample, Pellan *et al.*[29] have shown that while above about 35 K the magnetoresistance show a weak-field dependence, below about 30 K the field-induced resistivity changes sign, increases by orders of magnitude and displays a divergent behavior as a function of the field when $T_c$ is approached. Indicatively, $\Delta\rho/\rho^2$ appears to reach values well above 100 $(\Omega\ \mathrm{m})^{-1}$ at $T=17$ K, for a field around 7 T, while the same quantity is about 10 $(\Omega\ \mathrm{m})^{-1}$ above 35 K. The field and temperature dependence of magnetoresistance was found by Pellan *et al.*[29] to follow rather well the equation derived by Al'tshuler *et al.*,[30] with a term that takes into account the Maki-Thompson fluctuations.[20]

A crude estimate on the order of magnitude of $\Delta\rho/\rho^2$ is $\Delta\rho/\rho^2 = 10^2(\Omega\ \mathrm{m})^{-1}$ in correspondence to $\rho$ $(T=20$ K$) = 0.2 \times 10^{-3}(\Omega\ \mathrm{cm})$, yielding $(\Delta\rho/\rho) \approx 5 \times 10^{-4}$, still with rather negligible effect on the relaxation time. Furthermore, from the data in Fig. 7, the relaxation rates are not modified when the external field is reduced by a factor of 2.

### C. AF correlation effects

In the possible onset of antiferromagnetic (AF) correlation among the carriers, a decrease in the susceptibility in Eq. (10) would be feasible. The small contribution to the magnetic moment of the film due to the Pauli-type susceptibility might have covered the detection in the SQUID data of that onset while be detected in the relaxation measurements. However a drastic rise in AF correlation should imply a superconducting state similar to the one in cuprates, namely departing from the BCS scenario. At variance, the data for $2W$ in Fig. 8(a), resembling the ones in bulk NbN, are consistent with the conventional behavior for BCS superconductors.

### D. Effects of SC fluctuations on the density of states

According to the data in Fig. 8(b) and in the light of Eqs. (7) and (8), for $T$ approaching $T_c$ one could infer a decrease in the density of $5s$ Nb states at the Fermi level by a factor around 2, namely, to about 10% of the total density of states. Then the decrease in the Knight shift would be on the order of its value (around $-8$ kHz) and this, in principle, is compatible with the crude data that could be extracted on approaching $T_c$ [see Fig. 5(c)]. It should be remarked that the effect on $2W$ being observed only in the textured film and not in bulk NbN, then the depletion in the density of states has to be attributed to granularity-induced formation of singlets.

From the temperature dependence of the complex microwave conductivity[5] in thick NbN films a crossover from the three-dimensional to the two-dimensional fluctuations regime was observed on approaching $T_c$ from above. Correspondently the conductivity decreases, as expected. However, in accordance to the Aslamazov-Larkin model[20] for the SC fluctuations, the temperature range where significant effects occur is only a narrow one above $T_c$. It should be remarked that in the microwave measurements the external field is zero and so one could conjecture a field-induced enlargement of the temperature range where SC fluctuations are effective. The magnetic field could also have the effect of quenching the positive Maki-Thompson (MT) contribution to the relaxation rate, which in turn in zero field tends to cancel the negative density-of-states (DOS) contribution.[31]

Along this line of interpretation Lerner and Varlamov have suggested[32] to consider for our sample the negative DOS contribution to $2W$ for an effective one-dimensional (1D) dirty superconductor, the MT term being negligible in this case. The 1D character of the SC fluctuations has to be related to the structure of the effective grains of our sample, parallelepipeds of 100 Å $\times$ 100 Å for a length more than $10^{-4}$ cm thus resembling a wire. Close to $T_c$ (where the coherence length diverges) the 1D approximation should be valid. Then the correction to the relaxation rate reads

$$\Delta W \approx -W[16G_i^{(1)}/\sqrt{\varepsilon}] \tag{11}$$

with $\varepsilon = [T - T_c(H)]/T_c(H)$ while the Ginzburg-Levanyuk number is

$$G_i^{(1)} = 1.3/(k_F d)^{4/3}(k_B T_c \tau/2\pi h)^{1/3}. \tag{12}$$

From the electronic number density the Fermi wavevector is $k_F = (3\pi^2 n)^{1/3} = 1.87 \times 10^8$ cm$^{-1}$ and for grain size $d = 100$ Å, Eq. (11) can be rewritten as

$$\Delta W \approx -W\{2 \cdot 10^{-6}\}\tau^{-1/3}/\sqrt{\varepsilon}. \tag{13}$$

Then, by taking into account the DOS reduction the relaxation rate $W$ including SC fluctuations becomes

$$W'(T) \approx W\{1 - 2 \cdot 10^{-6}\tau^{-1/3}/\sqrt{\varepsilon}\}. \tag{14}$$

The solid line in Fig. 8(b) correspond to the above Equation, for an average correlation time $\tau = 10^{-16}$ s. This value might seem smaller than the typical time of flight of the electron in metals. However it should be taken into account that according to Reiss *et al.*[33] in well-crystallized films the grain-boundary scattering dominates the transport. Because of the

effects on the number density and quantum transparency when the grain boundaries are crossed by an electron during two successive scattering events, the mean-free path has to be written $\lambda_{eff}=\lambda\Gamma^{\lambda/d}$, where $\Gamma$ is the transmission probability while $\lambda/d$ is the number of grains per path ($d$ grain size). This corresponds to correct the average correlation time $\tau$ between scattering events in the form $\tau=\lambda\Gamma^{\lambda/d}/v_F$. $\Gamma$ seems to span a wide range, from $10^{-5}$ to $10^{-1}$,[2] but for NbN film a value around $10^{-1}$ is feasible. Indeed by Mathur *et al.*[34] from low-field magnetization measurement in NbN films an electronic mean-free path of 1.1 Å has been deduced, for Fermi velocity $v_F=2.10^8$ cm corresponding to $\tau$ just around $10^{-16}$ s. Thus the solid line in Fig. 8(b) can be considered to result from Eq. (14) with practically no adjustable parameter. The arise of the spin gap is therefore justified on the basis of SC fluctuations in 1D dirty regime coupled to the reduction in the time of flight of the electrons.

Regarding the 1D approximation, we would like finally to remark that one must be aware that such 1D condition applied to a parallelepiped (as above described) might be a crude approximation. In fact it could poorly be applied very far from $T_c$ while for $T$ close to $T_c$ one should enter in the critical region. Thus it is not expected a full agreement in the $T$ behavior between the experimental data and the theory developed within 1D approximation for the DOS term of SC fluctuations. On the other hand we stress that the most important aspect is the order of magnitude of the decrease in the relaxation rate expected from SF in the 1D regime on approaching $T_c$ [see Fig. 8(b), solid line, where one should take into account that the negative divergence is cut by entering in the critical region very close to $T_c$.]

## V. SUMMARIZING REMARKS AND CONCLUSIONS

A granular NbN film (111) textured of excellent structural and superconducting qualities has been studied by means of SQUID magnetization and $^{93}$Nb NMR spectra and relaxation measurements. Beside the intrinsic interest toward that type of superconducting system, one relevant aim of the research work was the comparison of the data with the findings in underdoped high-temperature cuprates superconductors. In fact, in the underdoped phase of cuprates NMR spin-relaxation measurements indicate the opening of a spin gap well above $T_c$ and correspondently magnetization measurements have revealed the presence of nonpercolating superconducting grains above the bulk $T_c$ exhibiting strong phase fluctuations of the order-parameter modulus. Furthermore, the temperature dependence of the resistivity is similar in underdoped cuprates and in NbN film at controlled granularity.[16,3,4] Finally, phase fluctuations of the order parameter just in the film used in the present work had been pointed out from previous measurements of the temperature dependence of the London penetration depth.

Part of the results obtained in our study could be expected once that the quality of the film could be ascertained. The superconducting state appears of $s$ wave BCS character and similar to bulk NbN, with a gap close to 3.5 $T_c(H)/2$ and with the occurrence of the coherence Hebel-Slichter peak just below the transition to the superconducting state. The phase fluctuations of the order parameter above $T_c$ have not been detected from magnetization measurements, thus yielding an indirect indication that the enhancement of the fluctuating diamagnetism, if any, is not as strong as in YBCO underdoped compounds.

The $^{93}$Nb NMR spectra show that is spite of the cubic structural symmetry, moderate electric field gradients at most of the Niobium nuclei are present, likely due to the grain boundaries. No structural phase transitions are reflected in the temperature dependence of the line width. Above about 40 K up to room temperature the $^{93}$Nb spin-lattice relaxation is strictly similar in our film and in well-prepared bulk NbN, with relaxation mechanism from electron scattering on the nuclei typical of the Fermi gas. At variance with bulk NbN, in the (111) textured film cooling below about 30 K the relaxation rate departs from the classical linear temperature dependence and opening of a spin gap resembling the effect in underdoped cuprates is actually detected. The depletion in the density of 5$s$ Nb states at the Fermi energy by a factor of 2 on approaching $T_c$ ($H$) can be used to justify the opening of the spin gap from the $^{93}$Nb relaxation rate. The concomitant effect that should occur in the Knigth shift is hard to put in evidence because of the small value that this quantity assumes with respect to the intrinsic NMR line width.

Some mechanisms in principle affecting the conventional scenario of the transport in the Fermi gas and then yielding spin-gap opening, have been considered. The depletion in the density of states due to SC fluctuations in the 1D condition coupled to the decrease in the effective correlation time of the electrons have been found to account for the spin-gap opening.

Sounding remarks arising from our experimental findings, with significant consequences also for the superconducting cuprates, are the following. First, the spin-lattice relaxation appears to be the only tool to provide clear and direct evidence of the reduction in the density of states around the Fermi level, irrespective of the microscopic mechanisms leading to it.

On the other hand the data in our granular NbN film suggest that the occurrence of the spin-gap phase in underdoped cuprates could be due more to granularity-related superconducting fluctuations rather than to the exotic mechanisms of magnetic origin elaborated in a variety of theoretical approaches. Further theoretical work along novel lines of interpretation suggested by these data should lead to better insights about the long-lasting problem of the pseudogap phase, including the one in high-temperature superconductors.[35]

## ACKNOWLEDGMENTS

Fruitful discussions with A. A. Varlamov are gratefully acknowledged. P. Carretta is thanked for his help and for suggestions in discussing the data. Useful correspondence with H. Nishihara is acknowledged.

[1] C. P. Poole, H. A. Farach, and R. J. Creswick, *Superconductivity* (Academic Press, 1995), Chap. 3, and references therein.
[2] For a recent paper on the properties of NbN films see K. Senapati, N. K. Pandey, Rupali Nagar, and R. C. Budhani, Phys. Rev. B **74**, 104514 (2006), and references therein.
[3] S. A. Wolf, D. U. Gubser, W. W. Fuller, J. C. Garland, and R. S. Newrock, Phys. Rev. Lett. **47**, 1071 (1981).
[4] R. W. Simon, B. J. Dalrymple, D. Van Vechten, W. W. Fuller, and S. A. Wolf, Phys. Rev. B **36**, 1962 (1987).
[5] T. Ohashi, H. Kitano, A. Maeda, H. Akaike, and A. Fujimaki, Phys. Rev. B **73**, 174522 (2006).
[6] G. Deutscher, Y. Imry, and L. Gunter, Phys. Rev. B **10**, 4598 (1974).
[7] I. V. Lerner, A. A. Varlamov, and V. M. Vinokur, Phys. Rev. Lett. **100**, 117003 (2008).
[8] M. R. Norman, D. Pines, and C. Kallin, Adv. Phys. **54**, 715 (2005).
[9] P. A. Lee, Rep. Prog. Phys. **71**, 012501 (2008).
[10] J. G. Naeini, X. K. Chen, J. C. Irwin, M. Okuya, T. Kimura, and K. Kishio, Phys. Rev. B **59**, 9642 (1999).
[11] G. V. M. Williams, J. L. Tallon, E. M. Haines, R. Michalak, and R. Dupree, Phys. Rev. Lett. **78**, 721 (1997).
[12] See A. Rigamonti, F. Borsa, and P. Carretta, Rep. Prog. Phys. **61**, 1367 (1998), and references therein.
[13] B. Ellman, H. M. Jaeger, D. P. Katz, T. F. Rosenbaum, A. S. Cooper, and G. P. Espinosa, Phys. Rev. B **39**, 9012 (1989); H. Takagi, B. Batlogg, H. L. Kao, J. Kwo, R. J. Cava, J. J. Krajewski, and W. F. Peck, Phys. Rev. Lett. **69**, 2975 (1992).
[14] A. Lascialfari, A. Rigamonti, L. Romanò, P. Tedesco, A. A. Varlamov, and D. Embriaco, Phys. Rev. B **65**, 144523 (2002); A. Lascialfari, A. Rigamonti, L. Romanò, A. A. Varlamov, and I. Zucca, *ibid.* **68**, 100505(R) (2003).
[15] Y. Wang, Z. A. Xu, T. Kakeshita, S. Uchida, S. Ono, Y. Ando, and N. P. Ong, Phys. Rev. B **64**, 224519 (2001); Y. Wang, Lu Li, and N. P. Ong, *ibid.* **73**, 024510 (2006).
[16] G. Lamura, J. C. Villegier, A. Gauzzi, J. Le Cochec, J. Y. Laval, B. Placais, N. Hadacek, and J. Bok, Phys. Rev. B **65**, 104507 (2002); J. C. Villegier, L. Vieux-Rochaz, M. Goniche, P. Renard, and M. Vabrè, IEEE Trans. Magn. **21**, 498 (1985); J. C. Villegier, B. Delaet, V. Larrey, P. Febvre, J. W. Tao, and G. Angenieux, Physica C **326-327**, 133 (1999); R. Chicault and J. C. Villegier, Phys. Rev. B **36**, 5215 (1987).
[17] E. Roddick and D. Stroud, Phys. Rev. Lett. **74**, 1430 (1995).
[18] V. J. Emery and S. A. Kivelson, Phys. Rev. Lett. **74**, 3253 (1995).
[19] L. Romanò, Int. J. Mod. Phys. B **17**, 423 (2003).
[20] A. Larkin and A. A. Varlamov, *Theory of Fluctuations in Superconductors* (Oxford Science, Oxford, 2005).
[21] See E. Bernardi, A. Lascialfari, A. Rigamonti, and L. Romanò, Phys. Rev. B **77**, 064502 (2008).
[22] H. Nishihara, Y. Furutani, S. Yokota, M. Ohyanagi, and Y. Kumashiro, J. Alloys Compd. **383**, 308 (2004).
[23] A. Rigamonti, Adv. Phys. **33**, 115 (1984).
[24] A. Narath, Phys. Rev. **162**, 320 (1967).
[25] M. Tinkham, *Introduction to Superconductivity* (McGraw-Hill, New York, 1996).
[26] C. P. Slichter, *Principles of Magnetic Resonance* (Springer-Verlag, Berlin, 1990).
[27] E. Ehrenfreund and T. H. Geballe, Phys. Rev. B **5**, 758 (1972).
[28] L. F. Mattheiss, Phys. Rev. B **5**, 315 (1972).
[29] Y. Pellan, G. Dousselin, J. Pinel, and Y. U. Sohn, J. Low Temp. Phys. **78**, 63 (1990).
[30] B. L. Al'tshuler, A. G. Aronov, A. I. Larkin, and D. E. Khmel'nitskii, Sov. Phys. JETP **54**, 411 (1981).
[31] P. Mosconi, A. Rigamonti, and A. Varlamov, Appl. Magn. Reson. **19**, 345 (2000).
[32] I. V. Lerner and A. A. Varlamov (private communication).
[33] G. Reiss, J. Vancea, and H. Hoffmann, Phys. Rev. Lett. **56**, 2100 (1986).
[34] M. P. Mathur, D. W. Deis, and J. R. Gavaler, J. Appl. Phys. **43**, 3158 (1972).
[35] I. V. Lerner, A. Rigamonti and A. A. Varlamov (unpublished).